Biomaterials 31 (2010) 2293–2301

Contents lists available at ScienceDirect

Biomaterials

journal homepage: www.elsevier.com/locate/biomaterials

Graft and diblock copolymer multifunctional micelles for cancer chemotherapy and imaging

Hsieh-Chih Tsai [a,1], Wei-Hsiang Chang [a,1], Chun-Liang Lo [c,1], Cheng-Hung Tsai [a], Che-Hau Chang [a], Ta-Wei Ou [d], Tzu-Chen Yen [e], Ging-Ho Hsiue [a,b,*]

[a] Department of Chemical Engineering, National Tsing Hua University, Hsinchu, 300 Taiwan, ROC
[b] Department of Chemical Engineering/R&D Center for Membrane Technology, Chung Yuan University, Chung Li, 320 Taiwan, ROC
[c] Department of Biomedical Engineering, National Yang Ming University, Taipei, 112, Taiwan, ROC
[d] Department of Chemical Engineering, National Central University, Taoyuan, 320 Taiwan, ROC
[e] Department of Nuclear Medicine and Molecular Image Center, Chang Gung Memorial Hospital and University, Taoyuan 333, Taiwan, ROC

ARTICLE INFO

Article history:
Received 14 October 2009
Accepted 18 November 2009
Available online 29 December 2009

Keywords:
Micelles
Drug delivery
Biocompatibility
Copolymer
In vivo test

ABSTRACT

Multifunctional mixed micelles that constructed from poly(HEMA-co-histidine)-g-PLA and diblock copolymer PEG–PLA with functional moiety was developed in this study. The mixed micelles had well defined core shell structure which was evaluated by TEM. The functional inner core of poly(HEMA-co-histidine)-g-PLA exhibited pH stimulate to enable intracellular drug delivery and outer shell of PEG-b-PLA with functional moiety Cy5.5 for biodistribution diagnosis and folate for cancer specific targeting were synthesized at the end of the polymer chain. The graft and diblock copolymer self assembled to nanospheres against water with an average diameter below 120 nm without doxorubicin, and an average diameter of around 200 nm when loaded with drug. From drug released study, a change in pH destroy the inner core to lead a significant doxorubicin(Dox) release from mixed micelles. Cellular uptake of folate–micelles was found to be higher than that of non-folate–micelles due to the folate-binding effect on the cell membrane, thereby providing a similar cytotoxic effect to drug only against the HeLa cell line. In vivo study revealed that specific targeting of folate–micelles exhibited cancer targeting and efficiency expression on tumor growth, indicating that multifunctional micelles prepared from poly(HEA-co-histidine)-g-PLA and folate–PEG–PLA have great potential in cancer chemotherapy and diagnosis.

1. Introduction

Successful anticancer drug delivery through systemic administration is crucial for cancer chemotherapy. Use of an appropriate drug carrier is needed for systemic administration to achieve selective accumulation of the chemotherapeutic drug in cancer tissue, and subsequently to provide an effective anticancer effect with a sufficient therapeutic index. Research on specific drug targeting on cancer cells is a challenging task [1,2]. This holds especially true for chemotherapeutic cancer treatment because most anticancer drugs cannot distinguish between cancerous and healthy cells. Among various strategies, one well-known approach is to chemically link to the micelle's outer layer specific ligands that can recognize the specific moiety on cancer cell membrane which will achieve receptor-mediated endocytosis. To further improve delivery efficiency and cancer specificity, a strong emphasis has been placed on developing drug carriers with active targeting ability. Moreover, tissue specificity is another issue for design of a safe carrier. Among various targeting moieties, such as peptide and antibody [3–6], which can be recognized and bind to specific receptors that are unique to cancer cells, the folate receptor is vastly over-expressed in several human tumor cells [7,8]. Although successful results have been reported for active targeting, few drug carriers exhibit the three functions of diagnosis, targeting, and therapy together on one micelle in vivo [9–14].

Recently, our group has reported multifunctional micelles containing a complete core and shell structure, prepared by mixing a graft copolymer and a diblock copolymer [15–17]. Two kinds of copolymer were used to reach the desired capabilities. Diagnosis and targeting were modified by linking cy5.5 and folic acid at the end of poly(ethylene glycol)-b-poly(D,L-lactide). Folic acids that exhibit high binding efficiency for epithelial tumors including ovarian, breast, and liver cancer have been proved. Graft

* Corresponding author. Department of Chemical Engineering, National Tsing Hua University, Hsinchu, 300 Taiwan, ROC. Tel.: +886 3 571 9956; fax: +886 3 572 6825.
E-mail address: ghhsiue@mx.nthu.edu.tw (G.-H. Hsiue).
[1] These authors contributed equally.

0142-9612/$ – see front matter © 2009 Elsevier Ltd. All rights reserved.
doi:10.1016/j.biomaterials.2009.11.059

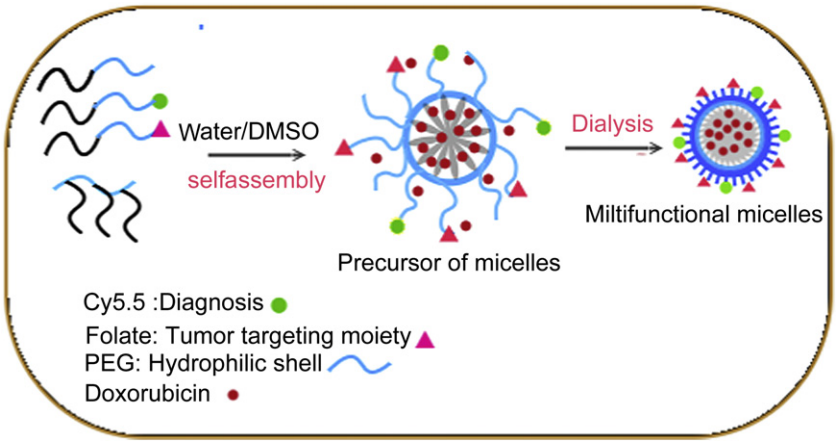

Fig. 1. Schematic representation the concept of loaded Doxorubicin by multifunctional micelles prepared by mPEG-b-PLA, Folate–PEG-b-PLA, Cy5.5–PEG-b-PLA, and Poly(Hema-co-Histidine)-g-PLA.

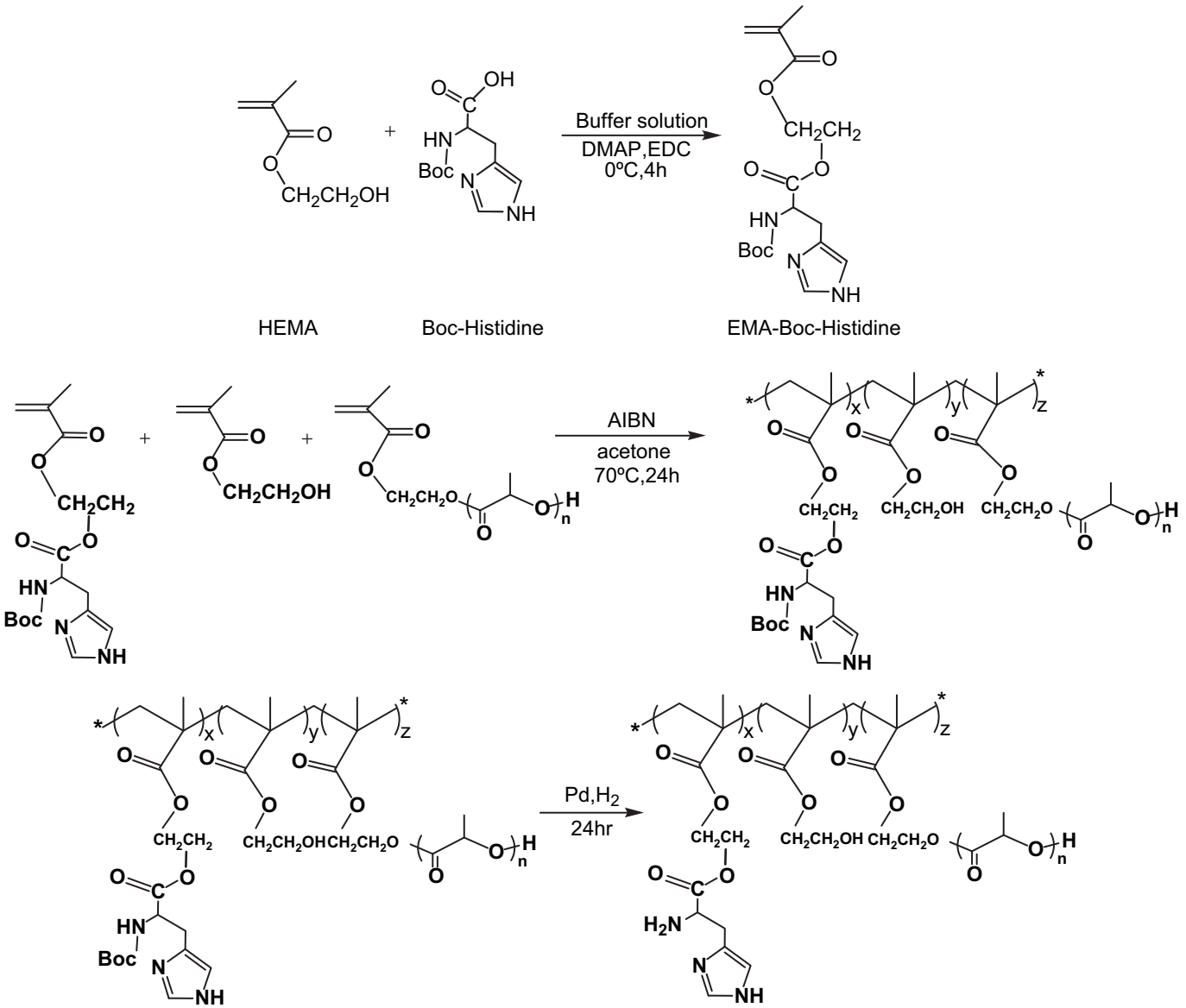

Scheme 1. Synthesis of Poly(HEMA-co-histidine)-g-PLA graft copolymer.

copolymer poly(2-hydroxyletheyl methacrylate-histidine)-g-poly-(D,L-lactide) was designed as the intracellular drug delivery agent for encapsulated anticancer drug doxorubicin (Dox). As shown in Fig. 1, this chemotherapeutic drug was loaded via self-assembly through hydrophilic interaction with copolymer. In order for the drug carrier to be used in the human body, the polymeric carrier must be biocompatibility, biodegradable, and bioabsorbable. We achieved this by incorporating histidine into the main chain poly(2-hydroxyethyl methacrylate) (poly(HEMA)) via esterification. Histidine has been used in therapeutic drug delivery formulation because its imidizole ring (pKb ~ 6.02) has a lone pair of electrons on an unsaturated nitrogen (NH of pyrrole) that confers pH-dependent amphoteric properties on the micelles [18,19]. The main chain of graft copolymer was constructed from poly(HEMA), which is one of the most important hydrogels in the biomaterials world, with many advantages over other hydrogels. These include water content similar to living tissue, inertness to biological processes, resistance to degradation, permeability to metabolites, and resistance to absorption by the body [20,21]. The biodistribution and targeting efficiency of multifunctional micelles was investigated in vivo using near infrared spectroscopy. Furthermore, we evaluated the therapeutic efficiency of Dox drug carrier by evaluating the anticancer effect in mice bearing HeLa tumors.

2. Materials

2.1. Materials

D,L-lactide and palladium were purchased from Lancaster. Stannous octoate, *N*-hydroxylsuccinimide, folic acid and 2,2′-azobisisobutyronitrile (AIBN) were purchased from Sigma. 2-hydroxylehtyl methacrylate (HEMA), 4-(dimethylamino)-pyridine (DMAP), 1-(3-dimethylaminopropyl)-3-ethylcarbodiimide (EDC), and *N*-(tert-butoxycarbonyl)-L-histidine were purchased from TCI. Cy5.5 mono NHS ester was purchased from GE Healthcare. α-t-butyloxycarbonylamino-ω-hydroxy-poly(ethylene glycol) (Boc-NH-PEG-OH) with Mw 3000 was purchased from Iris. D,L-lactide was further purified by recrystallization from THF twice before use. AIBN was purified by recrystallization from hexane and acetone, respectively. HEMA was purified by distillation in a vacuum. Other reagents were commercially available and were used as received.

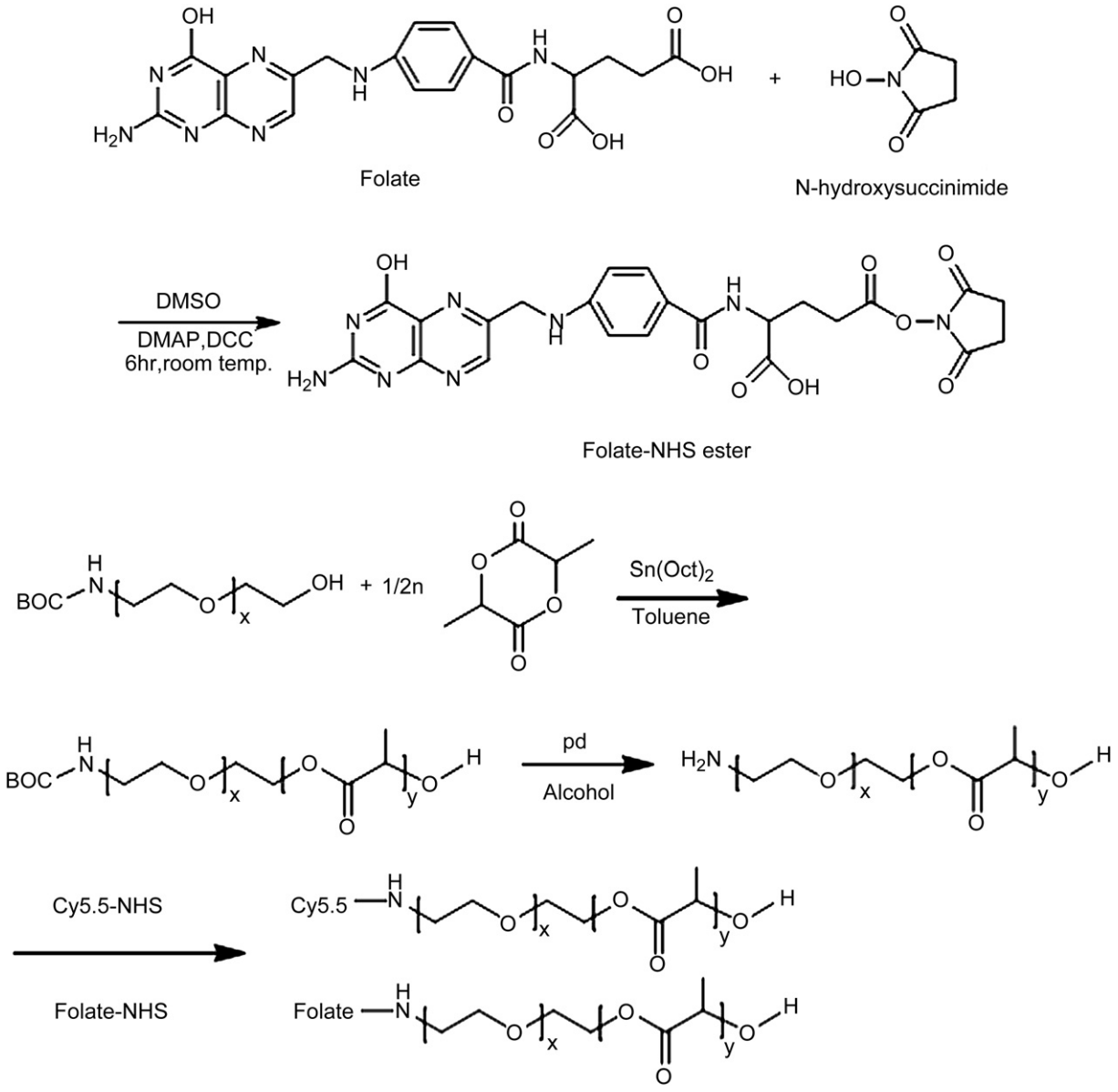

Scheme 2. Synthesis of Folate–PEG-b-PLA and Cy5.5–PEG–PLA diblock copolymer.

2.2. Synthesis of Boc-histidine–EMA (BOC-His–EMA)

Boc-histidine (1 mmol), HEMA (1 mmol), and DMAP (0.3 mol) were dissolved in buffer solution (0.01 M HEPES, 0.15 M NaCl, 3 mM EDTA) and added to a two-necked round-bottle flask with magnetic stirrer and addition funnel. EDC (1.5 mmol) was dissolved in RO water and added to the addition funnel. The reaction was carried out for 4 h in a 0 °C ice bath with slow drops of EDC solution. The product was characterized by ^{1}H NMR (d-chloroform). ^{1}H NMR ($CDCl_3$, ppm): δ 1.22 (s, 3H, CH_3–CH═C), δ 1.90–1.96 (t, 18H, $(CH_3)_3$–C–NH), δ 3.04–3.06 (s, 2H, CH_2 of His), δ 3.82–3.86 4.24–4.26 (t, 6H, $2CH_2$ of HEMA), δ 4.52–4.58 (s, H, NH of His), δ 3.04–3.06 (s, 2H, CH_2–histidine), δ 5.90–5.94 (s, H, CH═C), δ 6.76 (s, 1H, m-H of imidazole), δ 7.72 (s, 1H, o-H of imidazole).

2.3. Synthesis of poly(HEMA-co-histidine)-g-PLA

PLA with an end-cap of methacrylated group (PLA–EMA) was synthesized by ring-opening polymerization. D,L-lactide, HEMA, and toluene were added to a two-necked round-bottle flask with a magnetic stirrer. Stannous octoate was then added to start polymerization at 130 °C for 16 h under nitrogen. After polymerization, the reaction was terminated by adding 0.1 N methanolic KOH and precipitated twice from diethyl ether. PLA–EMA macromonomer (Mn 1400) with a methacrylated group at one end was obtained. Then, the poly(HEMA-co-Boc-histidine)-g-PLA graft copolymer was synthesized by traditional free radical copolymerization. PLA–EMA, HEMA, Boc-histidine–EMA, and AIBN were placed in a two-necked round-bottle flask with magnetic stirrer, and the mixture was dissolved in acetone. The reaction was conducted at 70 °C for 24 h under nitrogen. After polymerization, the product was purified by precipitation from diethyl ether twice to obtained polymers. Then the poly(HEMA-co-Boc-histidine)-g-PLA graft copolymer was dissolved in ethanol in the presence of Pd catalyst and reacted with hydrogen at room temperature for 24 h. The final product was characterized by ^{1}H NMR (acetone-d_6). δ 0.62–1.12 (m, CH_3 from HEMA, HEMA and histidine); δ 1.12–1.36 (m, CH_2 from EMA, HEMA, and histidine); δ1.4–1.56 (m, broad, CH_3 from PLA); δ1.4–1.56 (m, broad, CH_3 from NIPAAm; CH3 from EMA) d 3.6–4.0 (broad, CH from NIPAAm); d 5.12–5.19 (m, CH from PLA). The polydispersity index (PI) was 1.02 from GPC determination.

2.4. Synthesis of mPEG-b-PLA diblock copolymer

mPEG-b-PLA diblock copolymer was synthesized by ring-opening polymerization. mPEG with Mw 5000 and toluene were added to a two-necked round-bottle flask with a magnetic stirrer. Stannous octoate was then added to start the polymerization at 130 °C for 16 h under nitrogen. After polymerization the reaction was terminated by adding 0.1 N methanolic KOH and the product recrystallized from diethyl ether at 0 °C. The chemical structure of mPEG-b-PLA was characterized by ^{1}H NMR. ^{1}H NMR ($CDCl_3$, ppm): δ 1.41–1.59 (m, CH3 from PLA); δ 3.23 (s, CH3O from mPEG); δ 3.40–3.63 (m, CH_2CH_2O from mPEG); δ 4.16–4.21 (m, CH_2CH_2O from mPEG conjugated with PLA); δ 5.11–5.19 (m, CH from PLA). The polydispersity index (PI) was 1.2 from GPC determination (Scheme 1).

2.5. Synthesis of Folate–PEG–PLA

Boc-NH-PEG-PLA diblock copolymer was synthesized by ring-opening polymerization. D,L-lactide, Boc-NH-PEG (Mw = 4750, 3000) and toluene were added to a two-necked round-bottle flask with magnetic stirrer. Stannous octoate was then added to start the polymerization, which was carried out at 130 °C for 16 h under nitrogen. After polymerization, the reaction was terminated by adding 0.1 N methanolic KOH and the product recrystallized from dichloromethane and diethyl ether co-solvent. The Boc-NH-PEG-PLA was then reacted with H_2 in the presence of Pd catalyst at room temperature for 24 h to remove Boc. The final product was obtained after filtering out the Pd catalyst and precipitating from ether. Folate–PEG–PLA was prepared in a two step procedure: (1) carboxylation of folic acid with NHS to yield folate–NHS; (2) conjugation of NH_2–PEG–PLA(Mw 4750) with folate NHS to produce folate–PEG–PLA. The carbodiimide-activated folic acid can couple with either α or γ carboxyl group residue [22]. Reaction conditions were selected to favor linkage with γ carboxyl residue. Folic acid (1 g) dissolved in hydrous DMSO (30 ml) was reacted for 6 h with NHS (0.9 g) in the presence of DCC (0.5 g) under nitrogen at room temperature, and the major by product, 1,3-dicyclohexyllurea(DCU), was removed by filtration. Subsequently, the above NHS folate solution (3 ml) was added to a DMSO (5 ml) solution containing NH_2–PEG–PLA. The reaction was performed at room temperature for 10 h under nitrogen. The final product was purified by dialysis against deionized water for 24 h (molecular weight cutoff 2000 Da) and freeze-dried. A known amount of dried folate–PEG–PLA was dissolved in DMSO and characterized by UV–vis (Supporting information) and the concentration of conjugated folate also determined from a calibration curve.

2.6. Synthesis of Cy5.5–PEG–PLA

Cy5.5–PEG–PLA was synthesized by reacting the Cy5.5–NHS ester with NH_2–PEG–PLA(Mw 3000) dissolved in dimethyl sulfoxide at room temperature for 16 h. The final product was purified by dialysis against deionized water for 24 h (molecular weight cutoff 2000 Da) and then freeze-dried. The resultant Cy5.5–PEG–PLA was stored at 4 °C in the dark until use. Quantitative analysis of the amount of conjugated Cy5.5 to PEG–PLA was determined by measuring the fluorescence intensity (Scheme 2).

2.7. Preparation of Dox-loaded micelles

10 mg of poly(HEMA-co-histidine)-g-PLA graft copolymer and 20 mg mPEG–PLA diblock copolymer were dissolved together in 10 ml dimethylformamide (DMF) to prepare a polymer solution. Then 20 mg Dox–HCl was added to the polymer solution, together with triethylamine (TEA) with mole ratio 1.2:1. The hydrochloride of Dox was then removed by TEA, making the drug hydrophobic. The mixture was

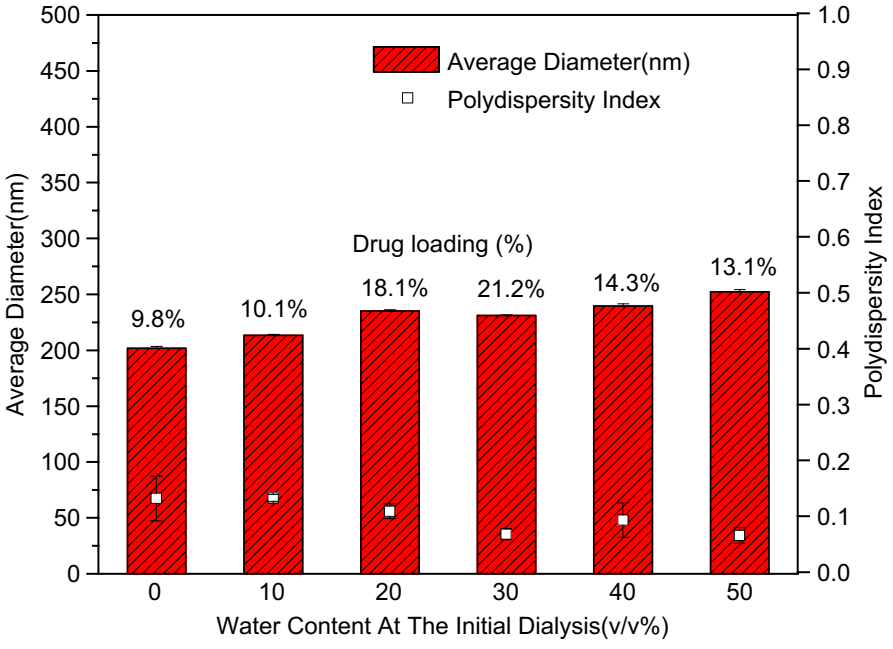

Fig. 2. Particle size, polydispersity and encapsulated Dox contents influence by changing the initial water contents before dialysis.

dialyzed against distilled water at 20 °C for 72 h, with the distilled water being replaced every 3 h. After dialysis, the solution of micelles was collected and frozen using a freeze dryer system to obtain dried micelles. Weighed amounts of mixed micelles were dissolved in DMSO at room temperature for 12 h, and then ultrafiltration (ultrafiltration membrane MWCO 1000, Millipore) was performed to extract samples to determine the Dox content of the mixed micelles by UV/Vis spectrometry at 485 nm with reference to a calibration curve of Dox in DMSO. The drug content of the mixed micelles was calculated using the following formula: drug content (% w/w) = (total mass of drug in mixed micelle)/(total mass of drug in mixed micelle + total mass of polymer in mixed micelle) × 100%. The particle size of Dox-mixed micelle was determined by dynamic light scattering using a sample in phosphoric acid buffer solution at pH 7.4 ($I = 0.01$) at a concentration of 0.1 mg/ml.

2.8. Drug release assay

The release behavior of mixed micelles loaded with Dox in pH 5.0 and pH 7.4 buffer solutions at 37 °C was determined by measuring, using a UV/Vis spectrometer at 485 nm in a time-course procedure, Dox isolated from a mixed micelle buffer solution (50 mg/l) by ultrafiltration (ultrafiltration membrane MWCO 10000, Millipore).

2.9. Internalization

Dox accumulated in HeLa cells was localized using a Carl Zeiss LSM5 PASCAL confocal laser scanning microscope (CLSM). The HeLa cells were seeded on coverslides for 24 h and were then treated with free Dox or Dox-mixed micelles. Dox-mixed micelles were washed with PBS to remove untrapped Dox twice before use. The concentration of Dox was about 10 mg/ml. After some time, the cells were washed twice with PBS, and then LysoTracker was added to the culture medium without FBS. After 3 h of incubation, the cells were washed with PBS and mounted on a slide with 4%w/w paraformaldehyde for CLSM observation. Fluorescence was observed by confocal microscopy at 488 nm excitation and using an LP filter of 590 nm for Dox detection. LysoTracker observation was also carried out using a confocal microscope.

2.10. In vivo optical imaging

Optical images were taken prior to and at selected time points after injection of Cy5.5 modified micelles. Mice were anesthetized by inhalation of 1.5% isoflurane in 1:2 O_2/N_2. The Cy5.5 modified micelles were injected intravenously through the tail vein. Optical imaging was performed, using an IVIS 100 imaging system, 24 h and 48 h after injection of Cy5.5 modified micelles. Optical imaging was acquired via the Cy5.5 filter channel using an exposure time of 1 s. The signal intensity was measured in defined regions of interest (ROI), which were similar locations within the tumor center. Relative specific targeting signal enhancement was calculated by using SI measurement: Relative Specific targeting (SI post in tumor)/(SI post in whole body).

2.11. In vivo antitumor activity

HeLa tumors was transplanted s.c. into the abdomen of female bulb-C mice (1×10^6 cells/0.1 ml). Seven days later (the size of tumor at this point was approximately 50 mm^3), the mice were treated i.v. once with free DOX, folate–micelles, micelles at doses of 5 mg/kg on a DOX basis ($n = 3$ for each group). The antitumor activity was evaluated in terms of the tumor size, which was estimated by the following equation: $V = (a) \times (b)^2/2$, where (a) and (b) are respective major and minor axes of the tumor measured with calipers.

3. Results and discussion

3.1. Polymer characteristics and biocompatibility of micelles

To introduce a functional group onto the surface of micelles, two diblock copolymers, folate–PEG_{5000}–PLA_{1550} and cy5.5–PEG_{3000}–PLA_{1550}, were fabricated as the shell of micelles. The functional end groups were synthesized by NHS and NH_2 coupling reactions. The chemical structure and PDI for each diblock copolymer were verified by H NMR, IR, UV and GPC, using dimethyl sulfoxide (DMSO) as an elution solvent. The core of the micelles was constructed from the hydrophobic chain of diblock copolymer and graft copolymer. In order to make the polymer suitable for biomedical applications, we redesigned the previous graft copolymer to make it biocompatible. In this study, a graft copolymer, poly(HEMA-co-histidine)$_{9082}$-g-PLA_{3874}, identified by ^{1}H NMR, IR and GPC as graft copolymer [HEMA]:[histidine]:[PLA] = 86.7:9.0:4.3, was synthesized. Empty mixed micelles preparation was the same as previously reported. The best size, diameter 114.6 ± 3.6 nm and PDI 0.252 ± 0.013, of empty mixed micelles was constructed from 33 mol% graft copolymer and 66 mol% diblock copolymer. These were responsive to pH change, with corresponding zeta potential measured as 2 ± 0.7 mv (see Supporting information). The cell viability assay showed that mixed micelles prepared from poly(HEMA-co-histidine)$_{9082}$-g-PLA_{3874} (IC_{50} = 18 200 ug/ml) against Hela cells had about 7.9-fold higher cell viability than the mixed micelles constructed from Poly-(NIPPAm-co-MAAc)$_{9970}$-g-PLA_{6150}(IC_{50} = 2300 ug/ml) which we previously reported [15–17].

3.2. Maximum Dox loading of micelles

Before loading the Dox into the polymeric micelles, Dox–HCl was stirred into 2 mol two mole ratio of TEA in DMSO, in order to detach the HCl and make the drug hydrophobic. Polymeric micelles with a core shell architecture are obtained from the self-assembly of amphiphilic copolymers in water. The concentration at which micellization occurs depends on factors such as the polymer composition, the hydrophobic/hydrophilic balance, and the

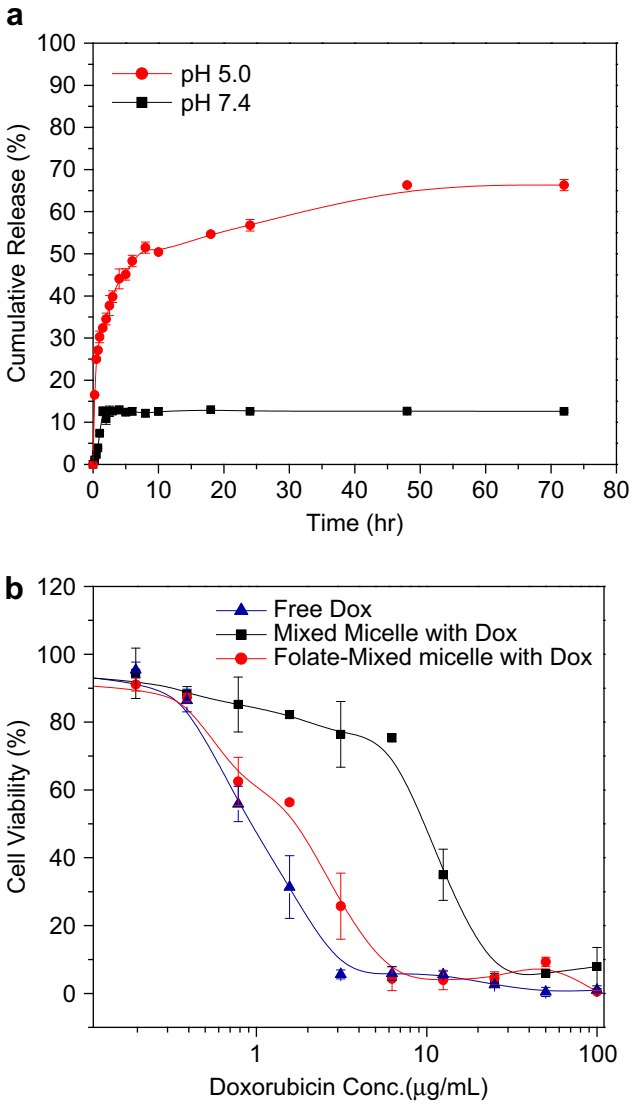

Fig. 3. (a) Released of Dox from multifunctional micelles under acidic (pH 5.0) and neutral (pH 7.4) condition at 37 °C. (b) Growth inhibition of Hela cells treated with various concentration of free Dox, micelles(Dox), and Folate–micelles(Dox).

polymer solvent interaction. Thus, in order to maximize the drug loading within the micelles, copolymer and hydrophilic Dox were mixed in DMSO/water solutions with different water fractions (0, 10, 20, 30, 40, 50 vol%) before dialysis. The results are shown in Fig. 2. The diameter and polydispersity index (PDI) were around 200 nm and 0.1 respectively. With addition of water into DMSO, we also observed a rise in the level of encapsulated Dox from 0% to 30 vol%. The maximum drug loading showed 21.2% drug loaded at initial water of 30 vol%. It seems that all the amphiphilic copolymer forms a precursor of micelles at this level of water added in DMSO solution. The enhanced size of the diblock and graft copolymer in the DMSO and water mixture can be attributed to swelling of hydrophobic cores in the organic solvent and water mixture, as it has been reported in other micelle formation [23]. This swollen core might provide a suitable environment for larger Dox molecules to interact with the hydrophobic segment, and the core at this concentration is expected to show a liquid-state characteristic to allow the drug to be loaded. The decreased loading of micelles with the water content between 40 and 50% can be attributed to the hydrophobic core being so tight at this concentration that Dox is

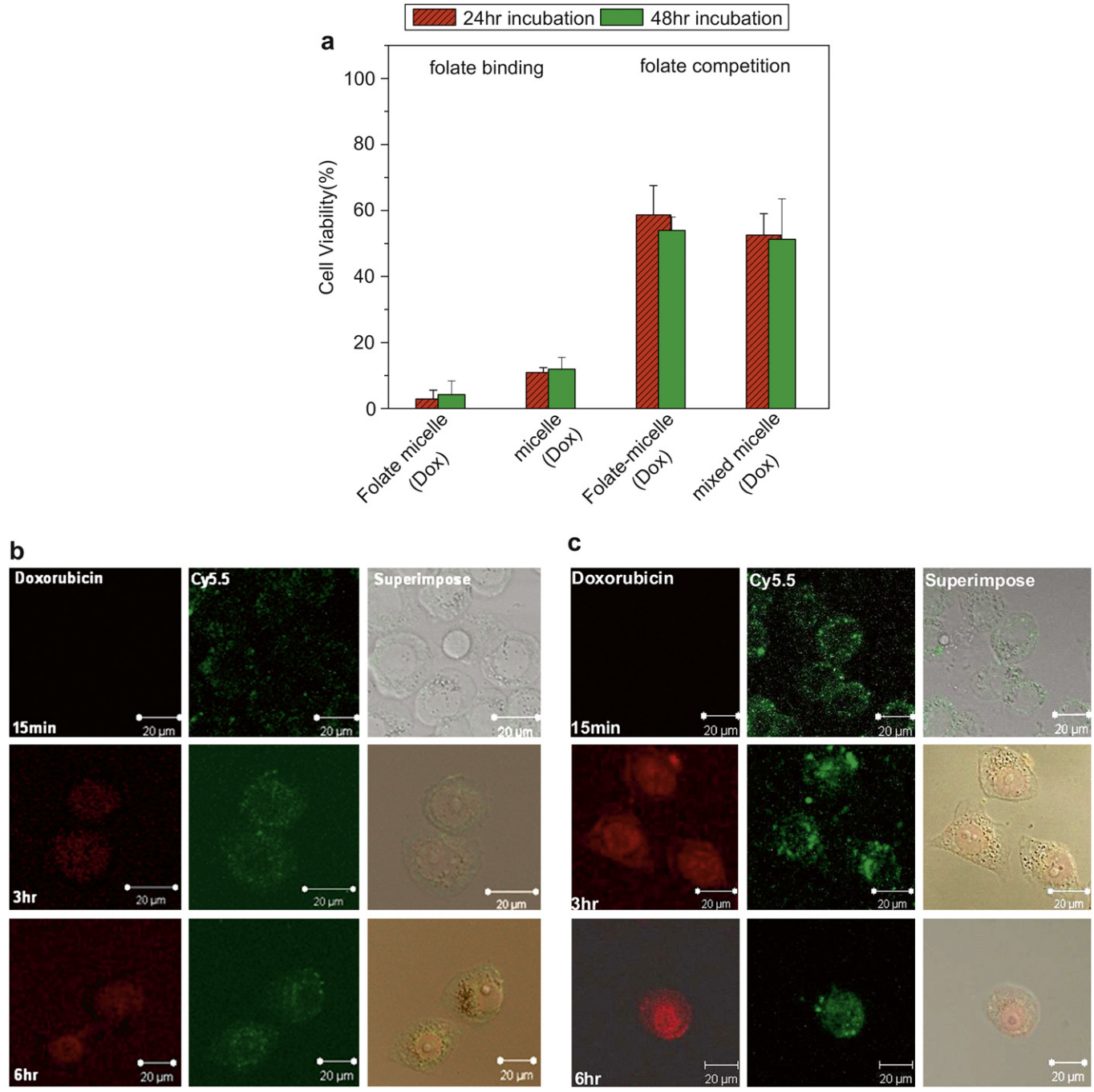

Fig. 4. Evaluation cell uptake of multifunctional micelles (a) micelles and Folate–micelles cytotoxicity after incubation with Hela cells for 24 and 48 h in the presence of 50 mM folic acid. Dox dosage was 50 ug mL^{-1} (b) Confocal images of Hela cells incubated with micelles at different incubation time period (c) Confocal images of Hela cells incubated with Folate–micelles at different incubation time period.

hardly able to get into the inner core of the micelles. By tuning the initial water content before micelle formation, we can obtain the maximum drug loading in the polymeric carrier, here, the maximum drug loaded micelles were chosen for the following experiment. The diameter of the drug loaded micelles was measured to be 231.1 nm, with polydispersity index 0.01 by laser light scattering technique. Hubbs et al. discovered that tumor vessels have a characteristic pore cutoff size that seems to maintain microenvironmental factors and the tumor milieu. In the tumor studied by their group, the pore cutoff size ranged between 380 and 780 nm [24]. Therefore, such Dox-loaded micelles were used to evaluate cancer targeting and therapeutic efficiency in vivo.

3.3. Drug release analysis and in vitro cell cytotoxicity

In order to evaluate the effect of stimulus response behavior on controlled drug delivery, the Dox release rate was studied under biologically simulating environmental buffer solutions (pH 7.4 and 5.0). Fig. 3 shows the Dox released from micelles at different pH levels. In neutral surroundings (pH 7.4), mixed micelles exhibited an initial burst effect, losing 10 wt%. At endosomal pH, i.e., pH 5.5, a burst release of Dox was observed throughout the first 10 h. During this period, almost 60% of encapsulated drug was released. HeLa cells are widely used for evaluating the interaction between folate-mediated drug delivery systems and cancer cells due to their high

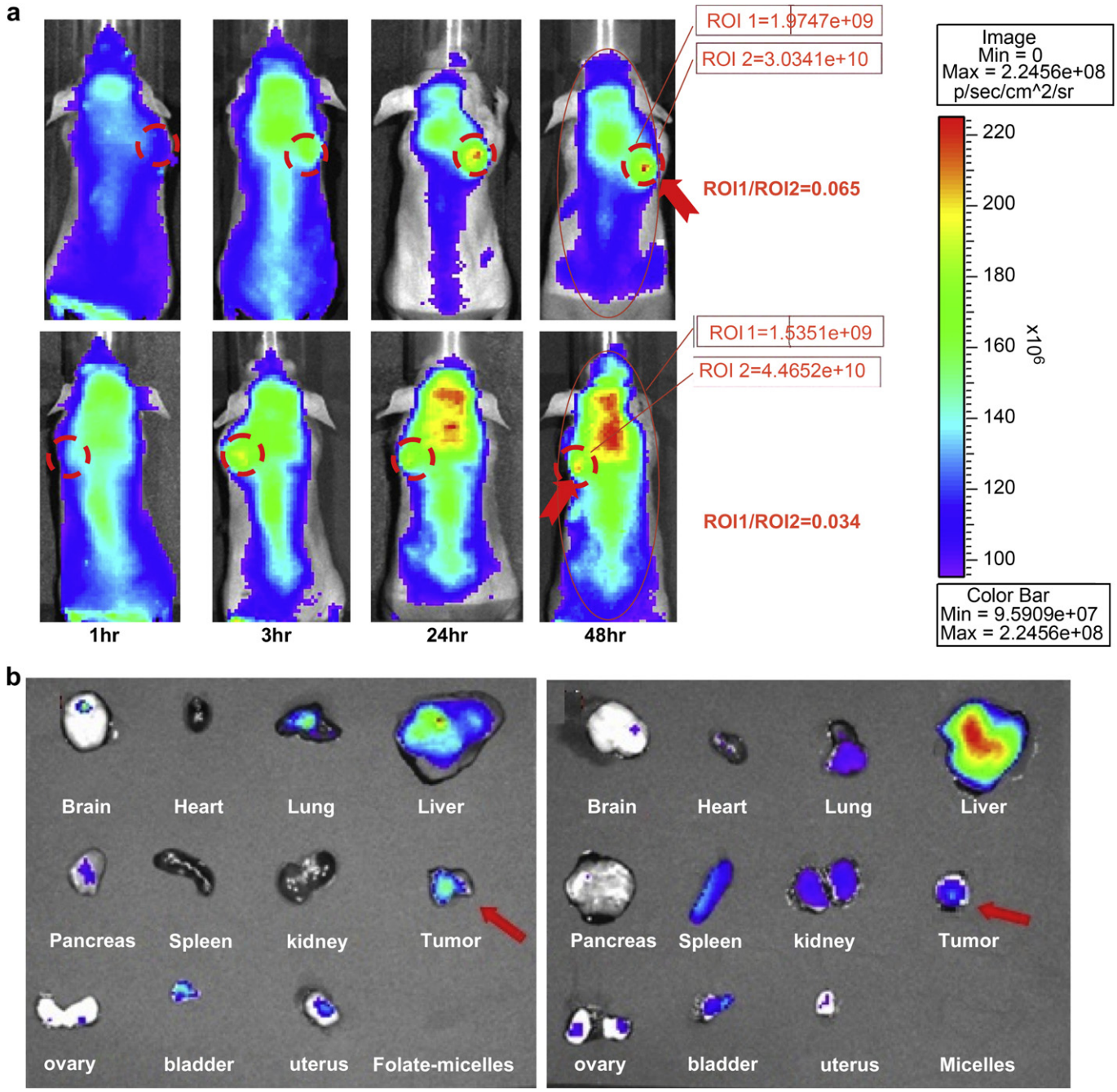

Fig. 5. (a) In vivo optical fluorescence imaging of Hela tumor xenografted nude mice administrated with micelles and Folae–micelles. Red circle specifies the location of tumor. (b) Photoimaging of several organs and tumor, which were taken after sacrifice (at 48 h post-injection) of the nude mice(injected with 5 mg/kg of Cy5.5 basis micelles). The fluorescence images were acquired with an exposure time 1s and used the Cy5.5 filter channel. The color indicates the relative fluorenscence.

affinity folate-binding protein (FBP) -binding effect [25,26]. The cytotoxicity of free Dox, micelles(Dox), and folate–micelles(Dox) for HeLa cells were analyzed by tetrazolium dye method (MTT). The inhibition concentration (IC_{50}) for free Dox, micelles(Dox) and Folate–micelles(Dox) was 0.92 ug/mL, 9.49 ug/mL, and 1.69 ug/mL respectively after 48 h incubation. Free Dox showed higher cytotoxicity than the micelles system due to passive diffusion of drug and directly caused cell death. Folate–micelles showed a comparable cytotoxicity to free Dox after 48 h exposure time, whereas the nonspecific target micelles had almost a 10 fold lower cytotoxicity than free Dox. It is unprecedented for folate–micelles to achieve as high cytotoxicity as free Dox despite their different internalization pathway. This result indicates that the use of folate–micelles may lower the effective dose of Dox, improving the safety of cancer chemotherapy.

3.4. Competitive assay and micelles uptake evaluation

Fig. 4a showed that the viability of HeLa cells after 24 and 48 h incubation with micelles or folate–micelles was compared. The folate–micelles showed lower cell viability than those without specific targeting moiety micelles. High cell viability for those micelles were obtained in the presence of 50 mM folic acid, showing that excess folic acid restrains the FPB-binding interaction between cell membrane and folate–micelle and proving that folate–micelles are taken up by the cell via a receptor mediated endocytosis pathway. Cellular uptake of folate–micelles and micelles were also evaluated by using confocal microscopy(Fig. 4b,c). By 15 min incubation time, the folate–micelles were rapidly taken up by the cells, as could be observed from the green light accumulated in cells from the Cy5.5 of the micelles. Intracellular drug release by folate–micelles and micelles could be visualized by intensity of red from Dox appearing at 3 h incubation time with HeLa cells. In the case of folate–micelles, Dox significantly localized in the nucleus instead of broadly distributing in the cytosolic compartment. This observation is clearly different from that of folate–micelles with FBP-binding effect showing high accumulation in HeLa cells compared with micelles in vitro.

3.5. Tumor accumulation

The time-dependent tumor accumulation of micelles in Hela-bearing nude mice was evaluated with near infrared spectroscopy. The diagnosis profiles of folate–micelles and micelles were clearly visualized by monitoring real-time NIR fluorescence intensity in the whole body (as shown in Fig. 5a) The NIR fluorescence of folate–micelles rapidly decreased in the whole body within 24 h post-injection, which may be due to specific targeting on tumor cells. From the calculation of relative light intensity of the tumor compared to light intensity for the whole body, relative accumulation of folate–micelles was (ROI1/ROI2 = 0.065) two fold higher than that of passive targeting micelles (ROI1/ROI2 = 0.034). Fig. 5b indicated that tissue distribution and tumor accumulation were evaluated from the NIR fluorescence image of dissected tumors and organs including brain, heart, lung, liver, kidney, spleen, pancreas, ovary, bladder, and uterus. In ex vivo NIR image at 48 h post-injection, strong fluorescence for micelles was observed in the liver. For folate–micelles, the decrease of light intensity in the liver and spleen suggest that micelles incorporated with the active targeting moiety are able to avoid recognition by RES and entrapment by hepatic sinusoidal capillaries, which are well-known filters for nanoparticles [27] In other words, the therapeutic efficiency could be maximized while minimizing unwanted side effects such as toxicity to other organs.

3.6. Antitumor activity of mixed micelles

The in vivo antitumor efficiency of free Dox, micelles(Dox) and folate–micelles(Dox) was validated in the HeLa-bearing mice. Micelles and drug were administered three times at 5 days interval on days 0, 5, 10, as represented by a red arrow in Fig. 6. Notably, the body weights of the mice slightly decreased during Dox administration with respect to control. The main side effects of doxorubicin include hypoleukocytosis, cardiac injury, liver and kidney toxicity. Mice administered Dox always show loss of weight [28–30]. However, the mice iv injected with micelles or folate–micelles showed no significant difference in body weight when compared with control, indicating that micelles reduced this side effect from drug toxicity to healthy cells. In the anticancer effect evaluation, mice administered micelles (DOX) showed approximately 60% tumor volume compared to the untreated control, which was a similar effect to administration of the drug only (Dox) at day 25. Although there is no difference in cancer therapy efficiency between Dox and micelle encapsulated Dox, the polymeric carrier would provide safer drug delivery. Importantly, folate–micelles inhibited tumor volume by up to 80% at day 25, a retarded tumor growth rate when compared with mice i.v. injected with Dox or

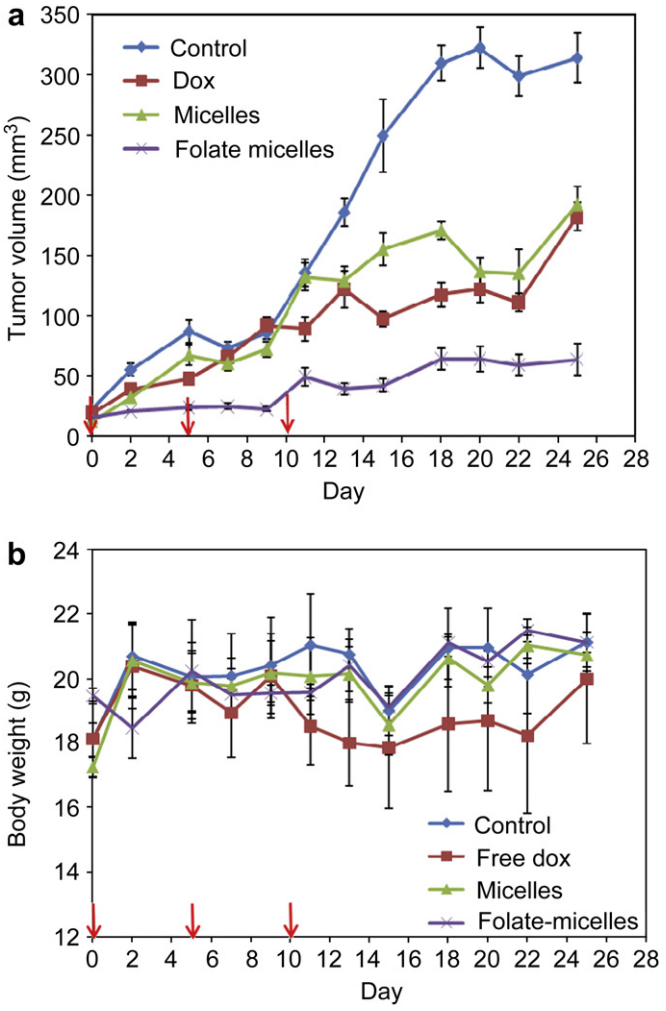

Fig. 6. Tumor growth inhibition test (a) and body weight change (b) of s.c. Hela xenografts in Balb/c nude mice(n = 3). Mice were injected i.v. with 5 mg/kg Dox equivalent dose. The administration were carried out 3 times with a 5 day interval in Hela-bearing mice.

micelles. The significant tumor inhibition effect can be attributed to the specific FBP biding effect of folate–micelles.

4. Conclusion

A new type of multifunctional micelle was constructed from Cy5.5–PEG–PLA, folate–PEG–PLA and poly(HEMA-co-histidine) -g-PLA as a polymeric carrier for tumor targeting delivery. In vitro and in vivo studies confirmed that selective targeting of micelles enhances specific uptake by cancer cells via a receptor mediated endocytosis pathway. Moreover, multifunctional micelles allowed detection of tumors by near infrared imaging, and at the same time delivery of sufficient amounts of anticancer drug that in turn were released from the micelles to exhibit anticancer activity. Consequently, folate–micelles showed exceptional antitumor effects without systemic toxicity. We anticipate that the aforementioned multifunctional micelles may be utilized in a distinct way to develop combined therapy and diagnosis for oncology.

Acknowledgments

The authors would like to thank the National Science Council of the Republic of China, Taiwan for financially supporting this work NSC 96-2628-b-007-001-MY2. TTY Biopharm Co. Ltd. (Taiwan) is appreciated for kindly providing the doxorubicin hydrochloride.

Appendix

Figures with essential colour discrimination. Many of the figures in this article have parts that are difficult to interpret in black and white. The full colour images can be found in the on-line version, at doi:10.1016/j.biomaterials.2009.11.059.

Appendix. Supplementary data

Supplementary information related to this article can be found at doi:10.1016/j.biomaterials.2009.11.059.

References

[1] Low PS, Antony AC. Folate receptor-targeted drugs for cancer and inflammatory diseases. Adv Drug Deliv Rev 2002;56:1055–8.
[2] Allen TM. Ligand-targeted therapeutics in anticancer therapy. Nat Rev Drug Discov 2002;2:750–63.
[3] Nasongkla N, Shuai X, Ai H, Weinberg BD, Pink J, Boothman DA, et al. cRGDfunctionalized polymer micelles for targeted doxorubicin delivery. Angew Chem Int Ed 2004;43:6323–7.
[4] Bertin PA, Gibbs JM, Shen CKF, Thaxton CS, Russin WA, Mirkin CA, et al. Multifunctional polymeric nanoparticles from diverse bioactive agents. J Am Chem Soc 2006;128:4168–9.
[5] Torchilin VP, Lukyanov AN, Gao ZG, Papahadjopoulos-Sternberg B. Immunomicelles: targeted pharmaceutical carriers for poorly soluble drugs. Proc Natl Acad Sci U S A 2003;100:6039–44.
[6] Sethurame VA, Bae YH. TAT peptide-based micelle system for potential active targeting anti-cancer agents to acidic solid tumors. J Control Release 2007;118:216–24.
[7] Ross JF, Chaudhuri PK, Ratnam M. Differential regulation of folate receptor isoforms in normal and malignant tissues in vivo and in established cell linesphysiologicand clinical implications. Cancer 1994;73:2432–43.
[8] Russell-Jones G, McTavish K, McEwan J, Rice J, Nowotnik D. Vitamin-mediated targeting as a potential mechanism to increase drug uptake by tumours. J Inorg Biochem 2004;98:1625–33.
[9] Bae Y, Jang WD, Nishiyama N, Fukushima S, Kataoka K. Multifunctional polymeric micelles with folate-mediated cancer cell targeting and pH-triggered drug releasing properties for active intracellular drug delivery. Mol Biosystems 2005;1:242–50.
[10] Prabaharan M, Grailer JJ, Pilla S, Steeber DA, Gong S. Folate-conjugated amphiphilic hyperbranched block copolymers basedon Boltorn (R) H40, poly(L-lactide) and poly(ethylene glycol) for tumor targeted drug delivery. Biomaterials 2009;30:3009–19.
[11] Sega EI, Low PS. Tumor detection using folate receptor targeted imaging agent. Cancer Metastasis Rev 2008;27:655–64.
[12] Hong G, Yuan R, Liang B, Shen J, Yamg X, Shuai X. Foltae-Functionalized polymeric micelles as hepatic carcinoma-targeted, MRI-ultrasensitive delivery system of anticancer drugs. Biomed Microdevices 2008;10:693–700.
[13] Zhang ZP, Lee SH, Feng SS. Folate-decorated poly(lactide-co-glycolide)-vitamin E TPGS nanoparticles for targeted drug delivery. Biomaterials 2007;28:1889–99.
[14] Bae Y, Nishiyama N, Kataoka K. In vivo antitumor activity of the folate-conjugated pH-sensitive polymeric micelle selectively releasing adriamycin in the intracellular acidic compartments. Bioconjug Chem 2007;18:1131–9.
[15] Lo CL, Huang CK, Lin KM, Hsiue GH. Self-Assembly of a micelle structure from graft and diblock copolymers: an example of overcoming the limitations of polyions in drug delivery. Adv Funct Mat 2006;16:2309–16.
[16] Huang CK, Lo CL, Chen HH, Hsiue GH. Multifunctional micelles for cancer cell targeting, distribution imaging, and anticancer drug delivery. Adv Funct Mat 2007;17:2291–7.
[17] Lo CL, Huang CK, Lin KM, Hsiue GH. Mixed micelles formed from graft and diblock copolymers for application in intracellular drug delivery. Biomaterials 2007;28:1225–35.
[18] Lee ES, Shin HJ, Na K, Bae YH. Poly(L-histidine)-PEG block copolymer micelles and pH-induced destabilization. J Control Release 2003;90:363–74.
[19] Lee ES, Na K, Bae YH. Polymeric micelle for tumor pH and folate-mediated targeting. J Control Release 2003;91:103–13.
[20] Tsuruta T. Contemporary topic in polymeric materials for biomedical application. Adv Polym Sci 1996;126:1–51.
[21] Antonsen KP, Bohnert JL, Nabeshima Y, Sheu M, Wu XS, Hoffman AS. Controlled release of protein from 2-hydroxyethyl methacrylate copolymer gels. Biomater Artif Cells Immobilization Biotechnol 1993;21:1–22.
[22] Dube D, Francis M, Leroux JC, Winnik FM. Preparation and tumor cell uptake of poly(*N*-isopropylacrylamide) folate conjugates. Bioconjug Chem 2002;13:685–92.
[23] Kohori F, Yokoyama M, Sakai K, Okano T. Process design for efficient and controlled drug incorporation into polymeric micelles carrier system. J Control Release 2002;78:155–63.
[24] Hobbs SK, Monsky WL, Yuan F, Roberts WG, Griffith L, Torchilin VP, et al. Regulation of transport pathways in tumor vessels: role of tumor type and microenvironment. Proc Natl Acad Sci U S A 1998;95:4607–12.
[25] Ogura H, Yoshinouchi M, Kudo T, Imura M, Fujiwara T, Yabe Y. Human parillomavirus type-18 DNA in so-called HEP-2-cells, KB-cells and FL-cells further evidence that these cells are HeLa-cell derivative. Cell Mol Biol 1993;39:463–7.
[26] Elwood PC. Molecular-cloning and characterization of the human folate-binding protein CDNA from placenta and malignant tissue culture(KB) cells. J Biol Chem 1989;264:14893–901.
[27] Moghimi SM, Hunter AC, Murray JC. Long-circulating and target-specific nanoparticles: theory to practice. Pharmacol Rev 2001;53:283–318.
[28] Zeidán Q, Strauss M, Porras N, Anselmi G. Differential long-term subcellular responses in heart and liver to adriamycin stress. Exogenous L-carnitine cardiac and hepatic protection. J Submicrosc Cytol Pathol 2002;34:315–21.
[29] Di DA, Ghiggeri GM, Di DM, Jivotenko E, Acinni R, Campolo J, et al. Lysyl oxidase expression and collagen cross-linking during chronic adriamycin nephropathy. Nephron 1997;76:192–200.
[30] Singal PK, Deally CM, Weinberg LE. Subcellular effects of adriamycin in the heart: a concise review. J Mol Cell Cardiol 1987;19:817–28.